GCOM-C/SGLI Sea Surface Temperature (SST) ATBD

Yukio Kurihara

JAXA/EORC

Ver. 3.0: Oct. 2021*

1 Introduction

Sea surface temperature (SST) is an important geophysical parameter associated with heat flux at the air-sea interface. JAXA provides an SST product generated from the data obtained with the Second-generation Global Imager (SGLI) onboard the Global Change Observation Mission -Climate (GCOM-C) satellite[1] (Fig. 1). The SGLI SST product version 3 is available at JAXA's G-Portal[2] since 2021. In version 3, cloud masking has been improved resulting increases in the total amount of available data in daytime. SST front issues found in previous versions have been improved for daytime SSTs.

This document presents the technical background of the SGLI SST product version 3. Data is outlined in Section 2, the algorithm is presented in Section 3, and its validation result is provided in Section 4. Lastly, currently recognized issues are presented in Section 5.

*Table A1 of change histories

[1]https://suzaku.eorc.jaxa.jp/GCOM_C/index.html

[2]https://gportal.jaxa.jp/gpr/

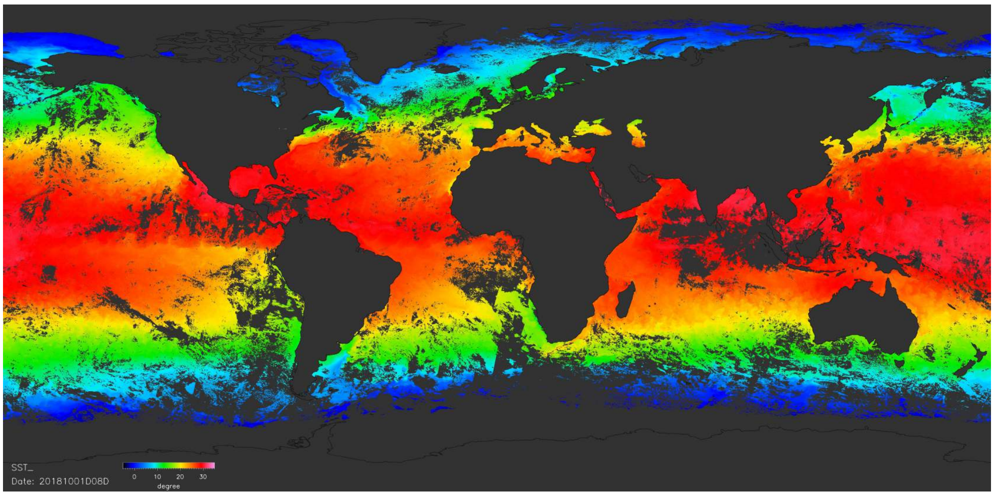

Figure 1. 8-day composite of SGLI SST at daytime from 1 to 8 Oct. 2018.

Table 1
GCOM-C specifications

Launch	23 December 2017 from Tanegashima Space Center
Launch Vehicle	HII-A
Weight	2,000 kg
Power	4 kw
Design Life	5 years
Orbit	Sun-synchronous
Altitude	798 km
Inclination	98.6 degrees
Equator crossing local time (descending)	10:30 ± 15 min.

Table 2
SGLI data for SST retrieval

Ch.	λ	IFOV	Cloud	SST
	$[nm]$	$[m]$	masking	determination
VN1	380	250 / 1000	no	no
VN2	412	250 / 1000	no	no
VN3	443	250 / 1000	no	no
VN4	490	250 / 1000	no	no
VN5	530	250 / 1000	no	no
VN6	565	250 / 1000	no	no
VN7	673.5	250 / 1000	no	no
VN8	673.5	250 / 1000	yes	no
VN9	763	250 / 1000	no	no
VN10	868.5	250 / 1000	no	no
VN11	868.5	250 / 1000	no	no
P1	670	1000	no	no
P2	865	1000	no	no
SW1	1050	1000	no	no
SW2	1380	1000	yes	no
SW3	1640	250 / 1000	yes	no
SW4	2210	1000	no	no
	$[\mu m]$			
T1	10.8	250 / 500 / 1000	yes	yes
T2	12.0	250 / 500 / 1000	yes	yes

2 Data

2.1 SGLI data

SST is determined with the split-window data (T1 and T2) obtained by SGLI onboard GCOM-C (Tables 1 and 2). The short-wave-length infrared data (SW2 and SW3) are used for cloud masking in daytime. The spatial resolution of SGLI can be switched between 250 m and 1 km. SGLI is used to observe lands and near-shore ocean areas with 250-m resolution and to observe open ocean with 1-km resolution. The swath width is 1,150 km for the VN and P channels and 1,400 km for the SW and T channels. The split-window data are preprocessed for destriping and denoising. This preprocess was introduced in the SGLI SST version 3. The destriping and denoising do not reduce the spatial resolution of the determined SSTs.

2.2 Ancillary data

The Merged Global Daily SST (MGDSST) is used in cloud detection at nighttime. MGDSST is objectively analyzed daily SST data provided by the Japan Meteorological Agency (JMA).

3 Algorithm

The algorithm is divided into two parts: the SST determination and the quality level (QL) decision. The first component determines SSTs for all pixels except for land. The second component assignes a QL to each determined SST.

Table 3
Bin for initial data and coefficients

Coordinate	Parameter	Interval
1	T_1	1.0 K
2	$T_1 - T_2$	0.1 K

3.1 SST determination

The SST algorithm is based on the quasi-physical method developed for Himawari-8 SST[3] [Kurihara et al., 2016, Yang et al., 2020]. Followings describe an outline of the algorithm. The detail of the method is discussed by Kurihara et al. [2021].

The formulas are

$$I_s = I_{s0} + \mathbf{a}\left(\mathbf{I} - \mathbf{I}_0\right), \tag{1}$$

$$T_b = \frac{hc}{K\lambda_1} \cdot \frac{1}{\ln\left(\frac{2hc^2}{\lambda_1^5 I_s} + 1\right)}, \tag{2}$$

and

$$T_s = \sum_{k=0}^{n} c_k {T_b}^k. \tag{3}$$

Here, I_s is the sea surface blackbody radiance at T1 and the subscript 0 denotes the initial value. $\mathbf{I}$ is the vector of the radiance observed at T1 and T2 and $\mathbf{a}$ is the coefficient vector. Eq. (2) is the inverse of the Planck function. Here, λ_1 denotes the central wavelength of T1. Eq. (2) converts the radiance to the blackbody temperature. In the conversion, the radiance is assumed to be the monochromatic. Eq. (3) translates T_b to SST (denoted by T_s), allowing for the Relative Sensor Response (RSR) of T1 into account.

The initial values and coefficients were generated for each bin (Table 3) for each satellite zenith angle, at 10° intervals using numerically simulated SGLI data. The simulation was made by performing the Radiative Transfer for TOVS (RTTOV) 10.2 RTTOV [Saunders et al., 2012] on numerical weather prediction (NWP) data. RTTOV is a radiative transfer model developed at the Numerical Weather Prediction Satellite Application Facility (NWP SAF) of the European Organisation for the Exploitation of Meteorological Satellites (EUMETSAT). The NWP data was provided by JMA.

3.2 Quality level

The quality level (QL) is decided for each determined SST based on the results of cloud masking. Due to the improved cloud masking, the QL decision flow has changed significantly from version 2. Figure 2 shows the cloud masking and QL decision flow. Each test and cloud probability are outlined below. QL is described in the 10-14th bits of the QA flag (Table 4). Note that quantitative uses are assumed about the SSTs with QL≥4 and that qualitative uses are assumed about those with QL≥3.

3.2.1 Smoothness test

The smoothness test divides the determined SST fields into coarse or smooth cells based on local uncertainty of the SSTs. Local uncertainty is calculated at each SST pixel from the variance of the SST gradients.

3.2.2 SST front test

The front test examines all SSTs in coarse cells. An SST recognized as part of a front is reorganized as part of a smooth cell. In version 3, a new front detection method was introduced for the front test.

[3]https://www.eorc.jaxa.jp/ptree/index.html

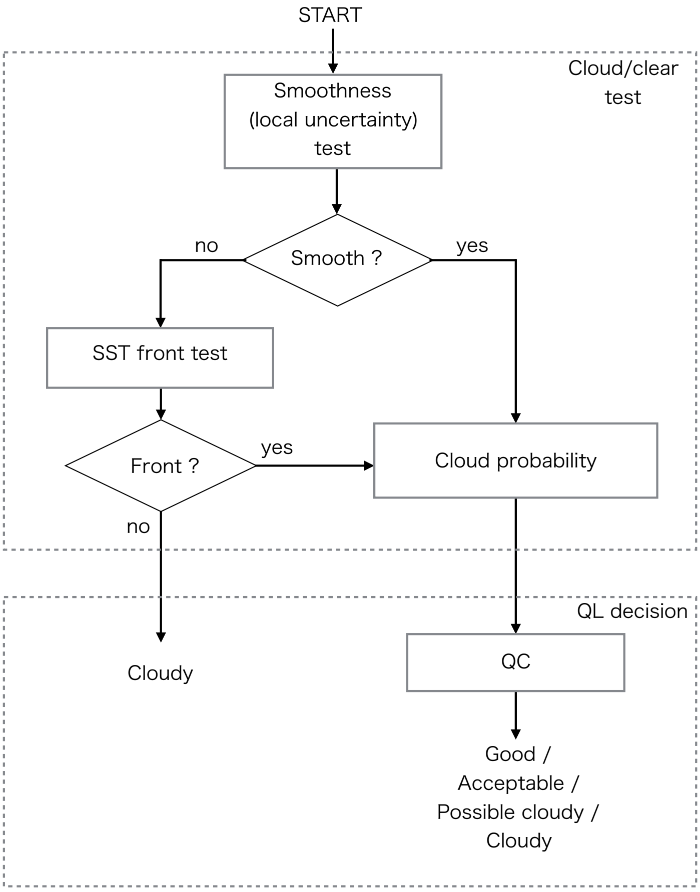

Figure 2. QL decision flow

Table 4
QA flag and QL

Bit	Description	Level-3 mask*	QL
0	Invalid data	1	
1	Land	1	
2	Rejected by QC	1	
3	Retrieval error	1	
4	Invalid data (TIR1)	1	
5	Invalid data (TIR2)	1	
6	reserved		
7	reserved		
8	1: daytime, 0: nighttime or no visible data		
9	Near Land		
10	Cloudy	1	1
11	Unknown clear/cloudy	1	2
12	Possibly cloudy	1	3
13	Acceptable		4
14	Good (daytime only)		5
15	reserved		

*) The level-3 mask denotes the bits which the level-3 statistics processing refers to. Data will be used for the level-3 statistics if all of the bits are zero.

3.2.3 Coast test (discontinued)

The coast test introduced for version 2 was removed in version 3. This is because of the cloud probability calculation improved by replacing VN8 with SW3.

3.2.4 Cloud probability

Cloud probability is calculated for each SST in each smooth cell. The cloud probability is the posterior probability derived by using prior information: SW2 and SW3 during the day and SGLI- and MGD- SSTs at night. The cloud probability calculation is based on the Bayesian inference method [e.g. Merchant et al., 2005]. The probability density functions (PDFs) are generated using the statistics derived from comparisons of SGLI SST and buoy data. The condition of the data, whether clear, cloudy, or mixed, depends on the difference between the collocated SGLI SST and buoy data.

3.2.5 QL decision

A QL is decided for each SST based on the determined cloud probability. QC is restricted to minimum. The thresholds for determining QL are different between day and night. Note that the highest QL is "Acceptable" for nighttime SSTs in version 3. This is because the cloud probabilities derived by using SST analysis are less reliable.

4 Validation

Figure 3 shows the statistics for SGLI SST version 3 for 2020. The statistics were calculated by comparing the drifting and moored buoys data with SGLI SSTs having good QLs. Buoy data were downloaded from the *in-situ* SST quality monitor (*i*Quam)[4] of the NOAA [Xu and Ignatov, 2014]. Each buoy data was compared with the nearest SGLI SST within a spatio-temporal window of 3 km×1 hr, centered on the buoy.

5 Issues

Following issues are recognized and waiting to be improved in the future.

1. Negative biases possibly dominate at SSTs above 300 K because of lower sensitivity to atmospheric water vapor.
2. In the nighttime, unstable accuracy of SST front detection possibly generates false clouds at and around SST fronts.
3. Because of insufficient information, cloud contamination can be conspicuous at nighttime.
4. Because of contamination of land, unnatural SSTs may be calculated along land/water boundaries.

[4]https://www.star.nesdis.noaa.gov/socd/sst/iquam/index.html

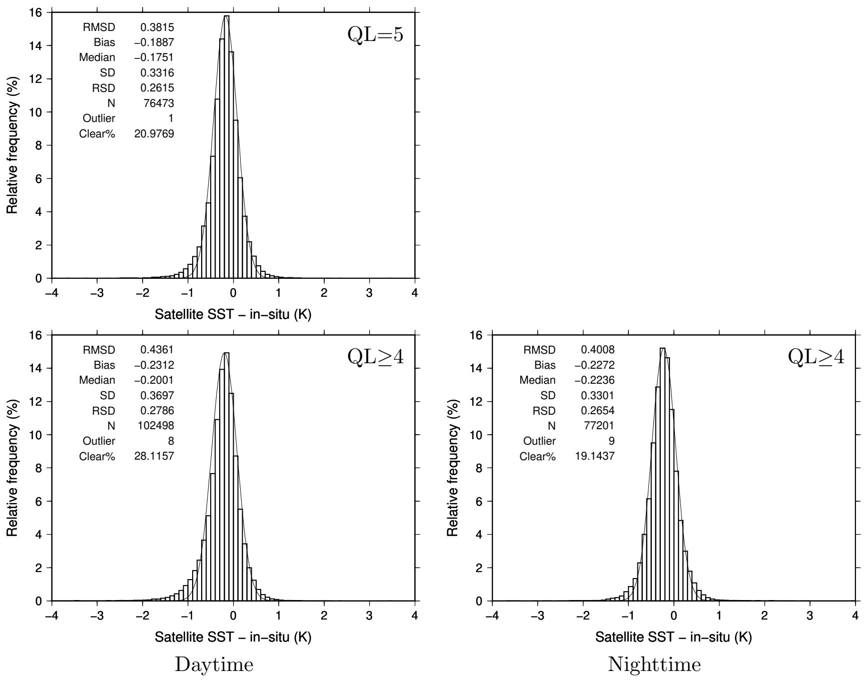

Figure 3. Relative frequency of the differences between SGLI and buoy data (SGLI−buoy). Statistics are calculated using the SGLI SSTs (QL=good) for 2020. The collocation window size is 1 hr × 3 km. rmsd: the root mean square difference, std: the standard deviation, rstd: the robust standard deviation, n: the total number of match-ups, outlier: the total number of the match-ups, s.t. |SGLI − buoy| > 4 K, and clear% : the ratio of the match-ups to all match-ups. Note that statistics were calculated for all match-ups including outliers.

References

Kurihara, Y., Murakami, H., and Kachi, M. (2016). Sea surface temperature from the new Japanese geostationary meteorological Himawari-8 satellite. Geophysical Research Letters, 43(3):1234–1240.

Kurihara, Y., Murakami, H., Ogata, K., and Kachi, M. (2021). A quasi-physical sea surface temperature method for the split-window data from the Second-generation Global Imager (SGLI) onboard the Global Change Observation Mission-Climate (GCOM-C) satellite. Remote Sensing of Environment, 257:112347.

Merchant, C. J., Harris, A. R., Maturi, E., and Maccallum, S. (2005). Probabilistic physically based cloud screening of satellite infrared imagery for operational sea surface temperature retrieval. Quarterly Journal of the Royal Meteorological Society, 131(611):2735–2755.

Saunders, R., Hocking, J., Rayer, P., Matricardi, M., Geer, A., Bormann, N., Brunel, P., Karbou, F., and Aires, F. (2012). RTTOV-10 science and validation report. EUMETSAT, NWPSAT-MO-TV-023, page 31.

Xu, F. and Ignatov, A. (2014). In situ SST Quality Monitor (iQuam). J. Atmos. Oceanic Technol., 31(1):164–180.

Yang, M., Guan, L., Beggs, H., Morgan, N., Kurihara, Y., and Kachi, M. (2020). Comparison of Himawari-8 AHI SST with Shipboard Skin SST Measurements in the Australian Region. Remote Sensing, 12(8).

Table A1
Change History

Version	Date	Description
1.0	Oct. 2018	
2.0	Jun. 2020	Cloud masking was improved for coastal areas and inland water. Fig. 2 (cloud masking flow) was modified along with a change to the cloud masking algorithm. Fig. 3 was updated. Fig. 4 was replaced with a time-series chart of bias and RMSD. Tables 3 (definition of LUT) and 4 (relative frequency of clear/cloudy) were modified. Table 5 (thresholds for QL) was removed. Table 6 (QA flag) was modified and renamed Table 5 (Table A2 for track changes). Substantial changes were made to descriptions including notations in Eq. (1).
3.0	Oct. 2021	Preprocessing for destriping and denoising of TIR data was introduced (Section 2). Cloud masking was improved. Section 3.2, Fig.2, and Table 4 were updated along with the changes to the cloud masking algorithm. Fig. 3 was updated. Fig. 4 was removed.

Table A2
QA flag (track changes)

Bit	Description
0	Invalid data
1	Land
2	Rejected by QC
3	Retrieval error
4	No data (TIR1)
5	No data (TIR2)
6	reserved
7	reserved
8	1: daytime, 0: nighttime or no visible data
9	Near Land
10	Cloudy
11	Unknown clear/cloudy
12	Possibly cloudy
13	Acceptable
14	Good (daytime only)
15	reserved